

Quantifying mass-loss rate reduction and porosity using the *Chandra* HETGS emission line profiles of ζ Puppis

David H. Cohen¹, Asif ud-Doula^{1,2}, Maurice A. Leutenegger³, Stanley P. Owocki²

ABSTRACT

We explore the joint effects of mass-loss rate reduction and isotropic porosity on symmetrizing x-ray emission line profiles, using the high signal-to-noise *Chandra* grating spectrum of ζ Puppis as a test case. We focus on one representative line – Fe XVII at 15.014 Å – and show that small values of τ_* and h_∞ are preferred. If τ_* is fixed at $\tau_* = 15$ (to approximate the value expected from the literature mass-loss rates), then $h_\infty \geq 4.5$ (68% confidence limit). This high- τ_* , high- h_∞ model approximates the line-profile morphology of the best-fit model – suppressing the blue-wing emission associated with high-optical-depth models – by having a large value of q ($q \approx 1$). Finally, as expected, a model that parameterizes porosity length as $h = h'r$ has a best-fit value of h' that is significantly lower ($h' \geq 1.01$ at the 68% confidence level) than the equivalent value of h_∞ .

1. Introduction

Note that although this document is formatted as a manuscript, at this point, it is more in the spirit of a memo to be circulated among collaborators.

The recent papers describing the effects of porosity on x-ray line profiles suggest that porosity's symmetrizing effects can explain (Oskinova, Feldmeier, & Hamann 2006) what previously had been interpreted as reduced continuum opacity (and, ultimately, attributed to reduced mass-loss rates)...or, perhaps, that it really *cannot* explain the surprisingly mild asymmetries and blue-shifts seen in the x-ray emission lines of O stars unless unrealistically large values of the porosity length are invoked (Owocki & Cohen 2006).

¹Swarthmore College Department of Physics and Astronomy, 500 College Ave., Swarthmore PA 19081

²Bartol Research Institute, University of Delaware, 217 Sharp Laboratory, Newark DE 19716

³Columbia University, Department of Physics and Columbia Astrophysics Laboratory, 550 W. 120th St., New York NY 10027

Here we report on fits we performed to the Fe XVII emission line at $\lambda = 15.014 \text{ \AA}$ in the *Chandra* HETGS spectrum of ζ Pup (MEG $m = +/ - 1$ orders). The HEG spectrum has negligible flux in this line. This line is representative - Kramer, Cohen, & Owocki (2003) fit it with a pure Owocki & Cohen (2001) line profile model having a best-fit $\tau_* = 1.0$. Our goals are to determine the extent to which opacity effects and porosity effects can be differentiated with real data. And to the extent they can be differentiated, which provides a better fit to the data. Even if the two effects cannot be differentiated, fitting real data will allow us to explore the trade-offs, or joint constraints, between opacity (via τ_*) and porosity (via h_∞). Specifically, we can answer the question, what values of the porosity length are required to fit the data, assuming that the literature mass-loss rates are correct?

2. The model and fits to the data

The line-profile model we use is the standard Owocki & Cohen (2001) four-parameter model (q , τ_* , $u_{\max}(R_*/R_{\min})$, and normalization), modified for the effects of isotropic porosity, using the effective opacity treatment of Owocki & Cohen (2006), according to eq. (11) in that paper. However, rather than assuming that the porosity length is proportional to the local radius, as $h = h'r$ (note that we assume in these notes that the values of the porosity length are in terms of the stellar radius), we assume that the clumps follow the wind velocity law (taken to be $\beta = 1$) – the so-called “stretch” porosity model (Owocki 2006). The local value of the porosity length thus scales as $h = h_\infty(1 - R_*/r)$. The porosity model is implemented in XSPEC in Maurice’s early-April version of *windprof* (note that *windprof* can include either the h' option or the h_∞ option). We include a continuum component in all of our modeling.

The data we fit is the first-order MEG only, over the interval $14.85\text{\AA} < \lambda < 15.13\text{\AA}$, which comprises 110 bins. We use the C-statistic to evaluate goodness of fit and to quantify the confidence limits on the fitted parameters.

The first fit we performed was the most general: all five parameters (q , τ_* , u_{\max} , normalization, and h_∞) were free to vary, as was the normalization of the continuum. The best-fit model parameters are in good agreement with the results of Kramer, Cohen, & Owocki (2003), including $\tau_* = 1.1$ (compare to their 1.0), and has the best-fit terminal porosity length value of $h_\infty = 0.00$. The best-fit parameters are summarized in Table 1 (quoted errors on the fit parameters are 68% confidence limits, throughout these notes). The best-fit model is shown, superimposed on the data in Fig. 1. The fit is very good. In fact, the very low C statistic value implies a rejection probability of only 3%. This is determined from fitting an ensemble of Monte Carlo simulated datasets and comparing the C statistic from the fit to the data to the distribution of C statistics generated from the Monte Carlo

simulations.

We should think about what it means that the fit is formally so good. We could say that the model is more detailed or complex than it needs to be. We could eliminate one or more of the free parameters. But we really have no *a priori* way to decide which ones are reasonable to eliminate (and what values we’d fix them at). In fact, if we were to eliminate one parameter, I would say the most reasonable thing would be to neglect porosity, functionally setting $h_\infty = 0$. But this is the best-fit value already. Another choice would be to fix $q = 0$, which is also very close to the best-fit value. Fixing $q = 0$ would, however, have implications for high- τ_* fits, as we will see below.

Given this best-fit model, we can quantify the uncertainties on the derived model parameters via the usual “ ΔC statistic” method. This will allow us to see how much larger than zero h_∞ can be before the model fit is significantly worse than the best-fit model. It will also enable us to see how much higher the derived τ_* value can be. We show the joint constraints on τ_* and h_∞ in Fig. 2. It can be seen from this figure that at the 90% (68%) confidence level, h_∞ can be almost as large as 3 (1.7). But interestingly, even if h_∞ is this large, τ_* does not have to increase by very much ($\tau_* \approx 3$ compared to the $\tau_* \approx 15$ expected from the literature \dot{M} and κ values).

I am actually somewhat surprised by this, as $h_\infty \approx 3$ seems like it should have a pretty big effect on τ_* . Maybe this is the difference between h' and h_∞ , and perhaps this difference is accentuated when τ_* is not very big. Because in this case the densest parts of the optically thin region are relatively close to the photosphere and thus $v < v_\infty$ and $h < h_\infty$. We can examine a model that is within the 90% confidence region but has relatively large values of τ_* and h_∞ . We show such a model in Fig. 3, with the corresponding fit parameters listed in Table 2. This fit, to my eye, looks perhaps a little worse than the best fit, but it still looks good. And indeed, as measured by Monte Carlo simulations, the rejection probability is just as low.

Next, we look at a model with a high τ_* value; something consistent with the literature mass-loss rate. Without a specific, detailed calculation of the x-ray opacity of the wind, we are guided by previously published opacities and related quantities for this and other stars’ winds. The expected wind optical depth under the assumption of a smooth wind is about an order of magnitude larger than the values found from fitting the Owocki & Cohen (2001) model to data, so we will choose $\tau_* = 15$ as the value expected for a smooth wind and literature mass-loss rate.

In Fig. 4 we show the best-fit model with τ_* fixed at 15, and all the other parameters free. The best fit model has $h_\infty = 5.5$. The lower limit on h_∞ is 4.5. So, a rather large

value of the porosity length is required if the mass-loss rate is not reduced¹. The model parameters of this fit are summarized in Table 3. Note that R_{\min} did not change very much, but q did. The best-fit value is $q = 0.82$. This high q value will de-emphasize the wings of the line. Note that a bump or flattening out of the profile can be seen near line center in this model. The model systematically overpredicts the flux in this part of the profile. It should be noted that the C statistic (like the chi-square statistic) is unaffected by correlations in the model-data deviations; by long runs of bins that all either over- or under-predict the level seen in the data. Some rank-order statistic (like the K-S statistic) might be more sensitive in this regard.

Note that this model is significantly worse than the best-fit model shown in Fig. 1 – the C statistic is 98 compared to 86 (implying $> 99\%$ significance). However, because the quality of the best fit is so good, the significantly worse fit still have a reasonable goodness of fit. So, in what sense can we rule out this high- τ_* , high- h_∞ model? I think we can only say that the low- τ_* , low- h_∞ model is *preferred* – with high statistical significance – over the high- τ_* , high- h_∞ model. Because the high- τ_* , high- h_∞ model requires a large increase in q , and because one might reasonably choose to fix $q = 0$ in order to keep the number of free model parameters small, it is instructive to look at a high- τ_* , high- h_∞ model with $q = 0$. The best-fit model with $\tau_* = 15$ and $q = 0$ fixed is shown in Fig. 5 and described in Table 4. Indeed this fit is significantly worse than the others we have shown. This seems to be due to an excess of emission on the blue wing, which is a universal characteristic of high- τ_* , high- h_∞ models (and which is suppressed by larger q values).

To assess the level of degeneracy among the model parameters, we compare three of the models we have discussed above, without convolving them with the instrumental response. This comparison is shown in Fig. 6. It can be seen from this figure that the models produce line profiles with quite similar, though not identical, morphologies. However, as we have just shown, the systematic differences in these morphologies can be distinguished with data of the quality of the ζ Pup MEG spectrum.

Finally, we have speculated above that the high value of h_∞ found in the high- τ_* ($\tau_* = 15$) model may be partly due to the nature of the stretch model, as parameterized by h_∞ . In Fig. 7 we show two suites of model calculations, which demonstrate that the symmetrizing effects of porosity are stronger in the linear model than in the stretch model, given equivalent values of h' and h_∞ . To quantify this difference, as constrained by data, we fit the same Fe XVII line at 15.014 Å with the linear porosity model. In Fig. 8 we show the best-fit model

¹Oskinova, Feldmeier, & Hamann (2006) find a value of $n_o = 2.6 \times 10^{-5} \text{ s}^{-1}$ for ζ Pup. Using their values for v_∞ and R_* , this value of n_o corresponds to $h_\infty = 6.4$.

and we display the fitted model parameters in Table 5. Note that all parameters were free in this model (q , u_{\max} , normalization, and h'), except for τ_* , which was fixed at $\tau_* = 15$, to facilitate a direct comparison to the high- τ_* , stretch porosity model shown in Fig. 4 and Table 3. Indeed, we find values of h' that are lower than the values we found for h_∞ by a factor of a few.

The results we report on here, for Fe XVII at 15.014 Å, are representative of what we find for other lines. We performed a comparable suite of fits to the Ne I line at 12.134 Å. Two of these fits, along with the confidence contours in the τ_* - h_∞ plane are shown in Fig. 9 and the fit parameters are listed in Table 6. While high- τ_* , high- h_∞ models are excluded at the 90% confidence level for this line too, the fits they provide are not as bad as the comparable fits to the Fe XVII line.

REFERENCES

- Kramer, R. H., Cohen, D. H., & Owocki, S. P. 2003, ApJ, 592, 532
- Oskinova, L., Feldmeier, A., & Hamann, W.-R. 2006, MNRAS, submitted (astro-ph/0603286)
- Owocki, S. P. & Cohen, D. H. 2006, ApJ, accepted
- Owocki, S. P. 2006, porosity notes for L. Oskinova,
(astro.swarthmore.edu/~cohen/projects/porosity/iso-vs-aniso-por.pdf)
- Owocki, S. P. & Cohen, D. H. 2001, ApJ, 559, 1108

Table 1. Fitted parameters for the best global model – all parameters free

parameter	value
q	$-0.02^{+.13}_{-.02}$
τ_*	$1.1^{+0.7}_{-0.1}$
h_∞	$0.00^{+1.7}_{-0.0}$
R_{\min}	$1.53^{+.11}_{-.11}$
C	82.95
rej. prob.	3%

Table 2. Parameters for a model with $\tau_* = 2$, $h_\infty = 2$ – all other parameters free

parameter	value
q	-0.04^+
τ_*	2
h_∞	2
R_{\min}	1.55^+
C	86.19
rej. prob.	3%

Table 3. Parameters for a model with $\tau_* = 15$ – all other parameters, including h_∞ , free

parameter	value
q	0.82^+
τ_*	15
h_∞	$5.5^{+1.2}_{-1.0}$
R_{\min}	1.73^+
C	98.44
rej. prob.	10%

Table 4. Parameters for a model with $\tau_* = 15$ and $q = 0$ – all other parameters, including h_∞ , free

parameter	value
q	0
τ_*	15
h_∞	6.7_{-}^{+}
R_{\min}	1.56_{-}^{+}
C	102.44
rej. prob.	21%

Table 5. Parameters for a linear porosity model with $\tau_* = 15$ – all other parameters, including h' , free

parameter	value
q	$0.40_{-.35}^{+1.05}$
τ_*	15
h'	$1.25_{-.24}^{+.25}$
R_{\min}	1.66_{-}^{+}
C	96.05
rej. prob.	11%

Table 6. Parameters for a stretch porosity model fit to the Ne X line at 12.134 Å: the right-most column lists the fit parameters for a model with τ_* fixed at $\tau_* = 15$.

parameter	value (all parameters free)	value ($\tau_* = 15$)
q	$0.16^{+0.24}_{-0.19}$	
τ_*	$1.89^{+3.52}_{-0.38}$	15
h_∞	$0.37^{+2.43}_{-0.34}$	4.10
R_{\min}	1.48^{\pm}	1.62^{\pm}
C	79.40	84.40
rej. prob.	14%	21%

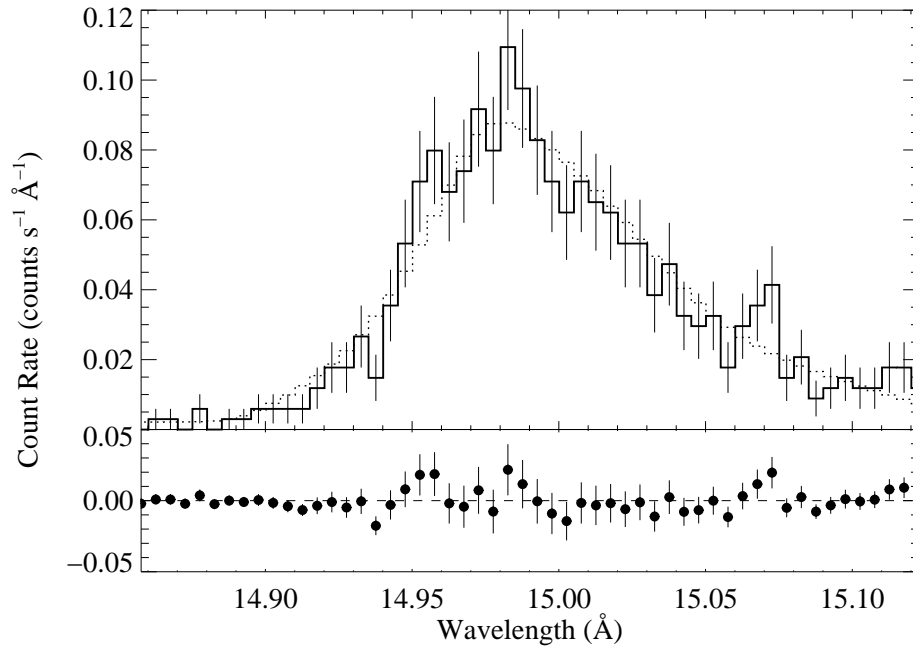


Fig. 1.— The global best-fit wind profile model for the Fe XVII line ($\lambda_{\text{lab}} = 15.014 \text{ \AA}$) measured in the MEG first order (negative and positive orders co-added). In this model, the free parameters were q , u_{max} , τ_* , h_∞ , and the normalization of the line profile, as well as the normalization of the power-law continuum model (for which we fixed the power-law index at $\alpha = 2$). The fit is formally very good. (fexvii_1501_windprof_best_q.thawed.ps)

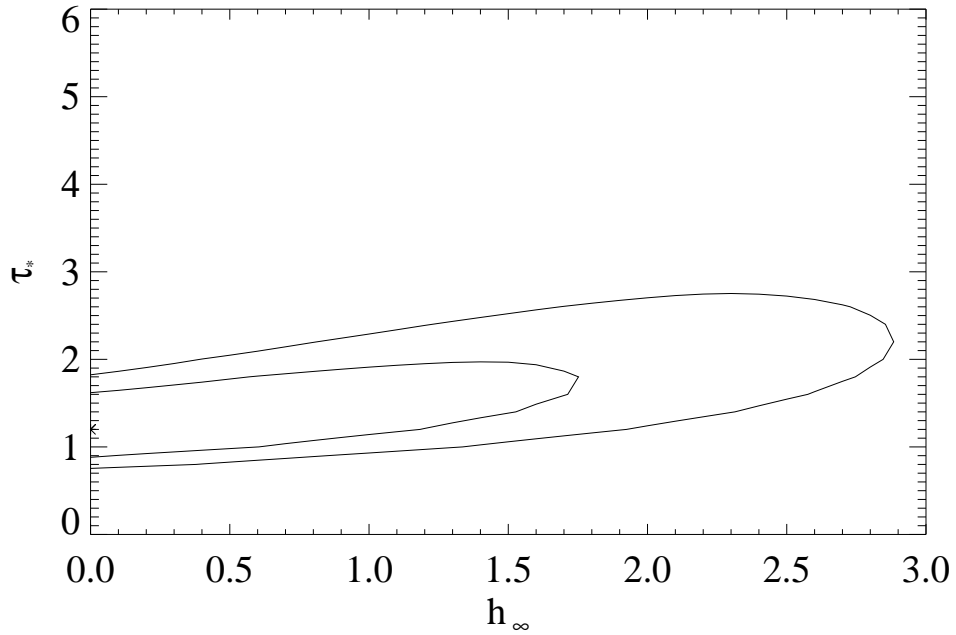


Fig. 2.— The 68% and 90% confidence regions for two parameters of interest ($\Delta C = 2.30, 4.61$). The calculated grid is 20 by 20, and for each of the 400 models, the other parameters (q , u_{\max} , normalization, and the normalization of the power-law continuum) were free to vary until a best-fit model for those values of τ_* and h_∞ was found. The best-fit value on the grid is indicated with an asterisk. (fexvii_1501_thawed_q.ps)

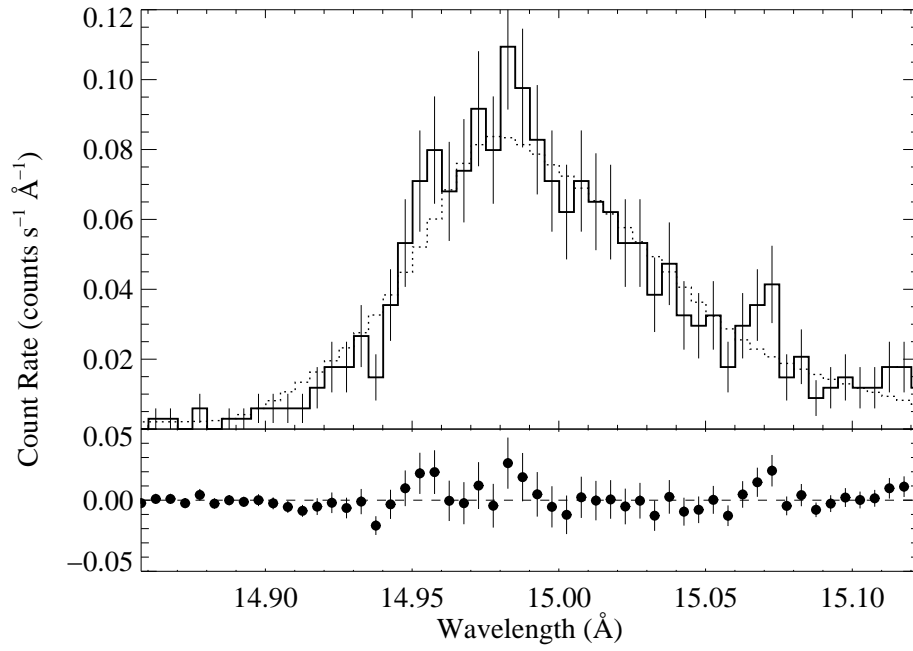


Fig. 3.— This fit has two additional parameters fixed, and represents a marginally acceptable fit, as compared to the best-fit model. (fexvii_1501_windprof_moderate_q_thawed.ps)

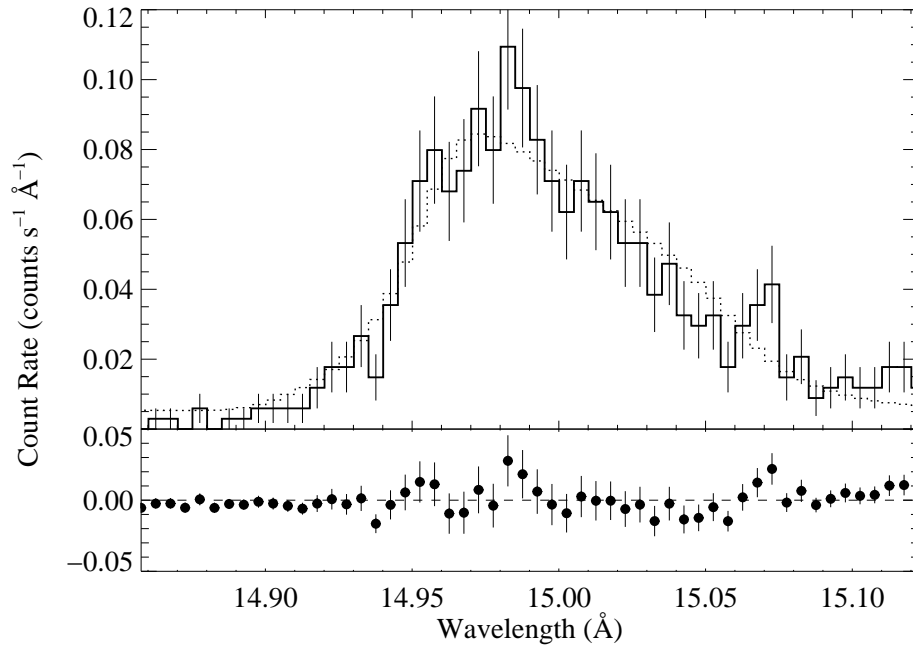


Fig. 4.— This fit has τ_* fixed at 15, with all the other parameters being free. The fit is significantly worse than the best-fit model shown in Fig. 1. (fexvii_1501_windprof_best_tau_15.ps)

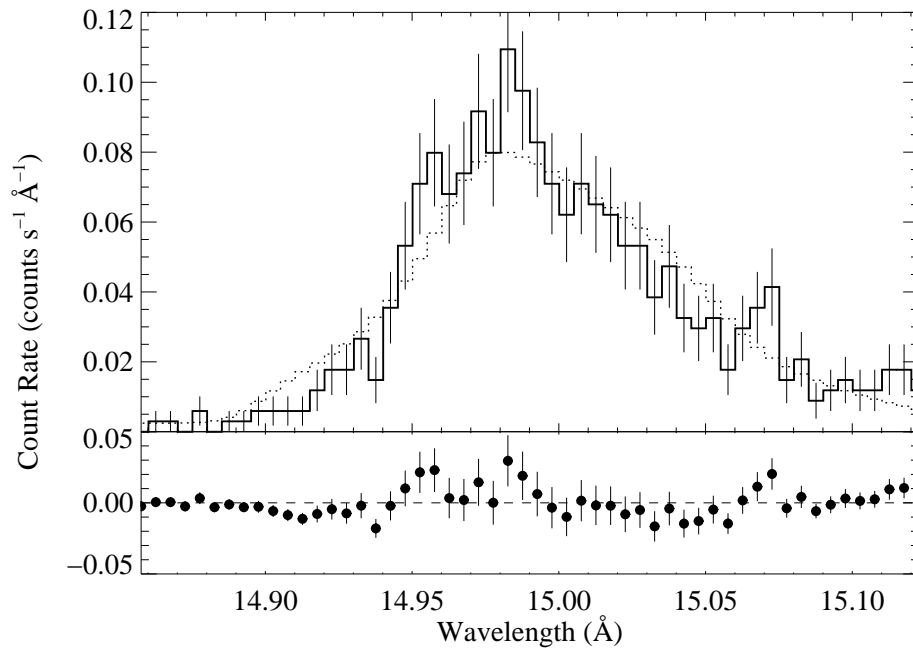


Fig. 5.— This fit has τ_* fixed at 15 and q fixed at 0, with all the other parameters being free. Note the bump on the blue wing of the model. The fit is significantly worse than the best-fit $\tau_* = 15$, q free model shown in Fig. 4. Clearly there are systematic deviations between this model and the data. (fexvii_1501_windprof_best_q_fixed_hinf_thawed.ps)

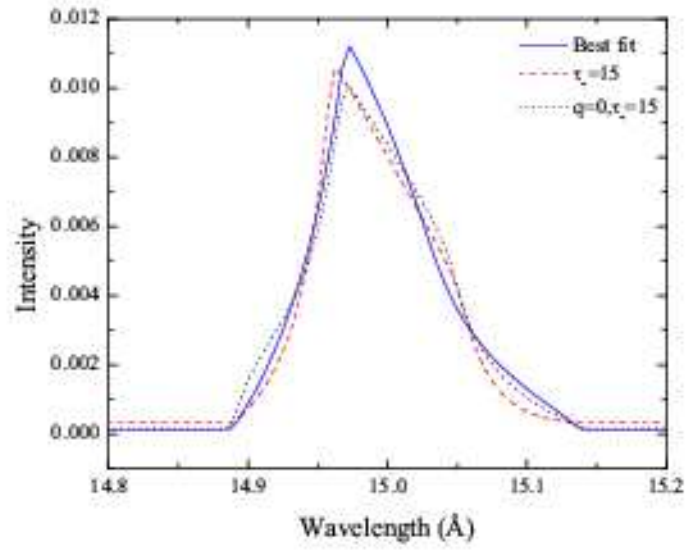


Fig. 6.— Three of the models we fit to the 15.014 Å line: the global best fit, the model with $\tau_* = 15$, and the model with $\tau_* = 15$ and $q = 0$. (best_fit.eps)

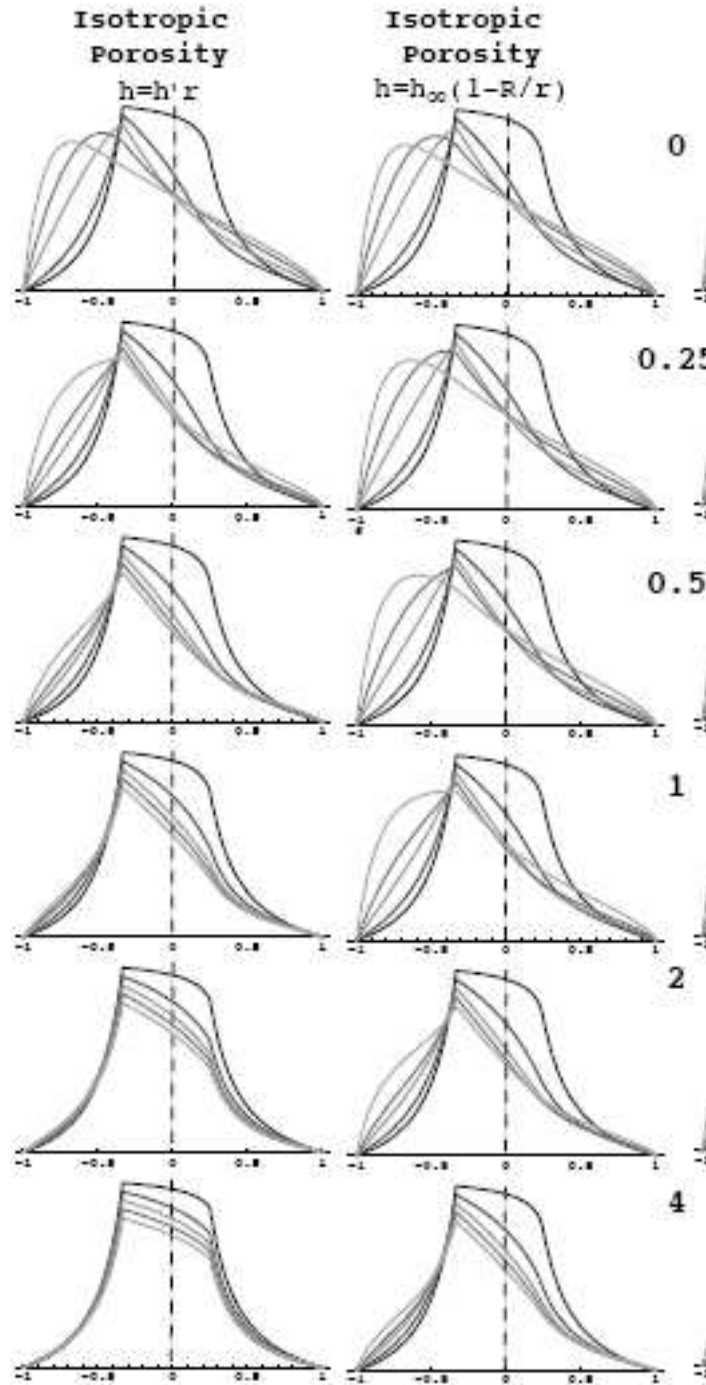


Fig. 7.— Suite of models comparing the linear treatment of porosity (left-hand column) to the stretch treatment (right-hand column) for a series of values of h' (left) and h_∞ (right), respectively. In each panel, different values of τ_* are shown. All models assume $R_{\min} = 1.5R_*$ and $q = 0$. (stan_suite.eps)

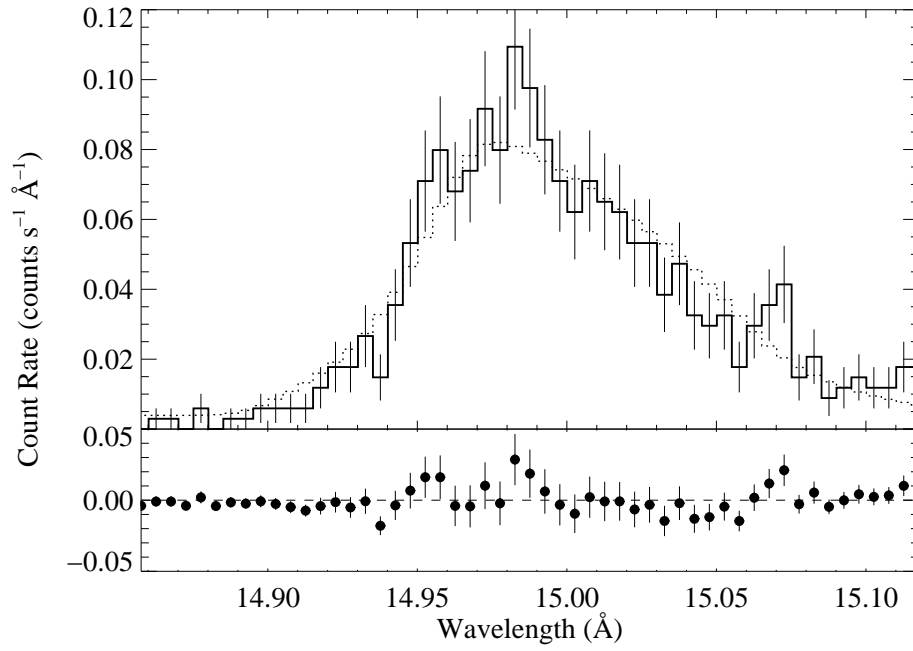


Fig. 8.— Best-fit *linear* porosity model, with $\tau_* = 15$ fixed and all other parameters free. (fe_xvii_1501_best_hprime_thawed.ps)

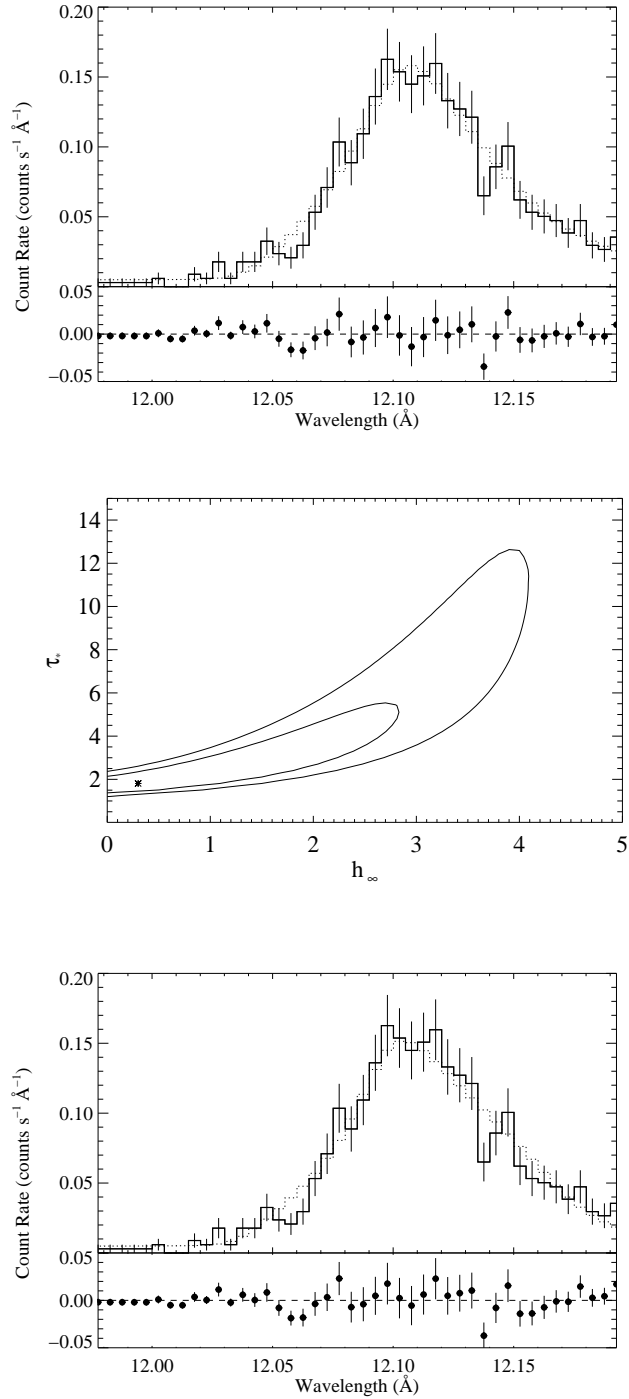


Fig. 9.— Best-fit stretch porosity model – with all parameters free – fit to the Ne X Lyman-alpha line at 12.134 Å (top). We also show the 68% and 90% confidence limits for this fit (middle) and a fit to the same line with a stretch porosity model for which we fixed $\tau_* = 15$ (bottom). (nex_1213_best_fit.ps; NeX_1213_hinf_vs_tau.ps; nex_1213_best_tau_15.ps)